

A. ZADE<sup>1</sup>, B. SRIDHAR BABU<sup>2</sup>, R.R.P. KUPPUSAMY<sup>1\*</sup>

## PROCESS OPTIMIZATION USING CUCKOO SEARCH ALGORITHM FOR THE MANUFACTURING OF RESIN TRANSFER MOULDED COMPOSITE PARTS

An in-house coded cuckoo search (CS) optimization algorithm integrated with a finite element simulation model was developed for resin transfer moulding (RTM) process optimization. At first, the mould filling and curing phases, the vital stages of the RTM process were modelled in the COMSOL multi-physics simulator for RTM6 resin – carbon fibre reinforced composite part. Then, the model was imported to the CS optimization algorithm scripted in MATLAB using the COMSOL live link for MATLAB. The CS algorithm was developed for the minimization of dry spot content by finding the optimal positions of gates and vents during the mould-filling stage and the minimization of the thermal gradient by finding the optimal mould temperature during the curing stage. From the optimization results, there was a decrease in dry spot content and thermal gradient with an increase in generations. With the generations, converged-stable-optimal solutions were obtained. A dry spot content of 3% for one gate and one vent and 0.56% for two gates and one vent was obtained for two-dimensional and three-dimensional composite plates, respectively. From the curing phase optimization results, a minimum thermal gradient of 0.86 K with 98.1% degree of cure was obtained for the optimal mould temperature of 433 K. The developed CS algorithm predicted the better-automated mould-fill and cure phase optimal solutions for the studied composite part.

*Keywords:* Resin Transfer Moulding; Cuckoo Search Algorithm; Mould-Filling; Curing; Finite Element Simulation

### 1. Introduction

Composite materials have gained significant importance in the aerospace and automotive industries due to their combination of lightweight and high strength, as well as their eco-friendly features, resulting in improved fuel efficiency and decreased CO<sub>2</sub> emissions. Despite their numerous benefits, the utilization of these composite components remains restricted due to the expenses associated with materials and manufacturing methods. The adoption of Liquid Composite Moulding (LCM) techniques has seen a rapid rise in the creation of aircraft composite parts, driven by advancements in tool design, process simulation, and modern equipment. Resin Transfer Moulding (RTM), a category of LCM, stands out as a widely employed manufacturing process for crafting composite parts for various applications [1]. RTM involves successive stages of mould filling and curing, either with or without external heat [2,3]. During the mould-filling phase, the pressurized resin is injected into the mould via designated injection ports ultimately leading to the complete saturation of the fibre preform [4]. Given the intricate nature of composite parts characterized by their complexity and scale, the utilization

of multiple injection ports and strategically positioned vents emerges as a crucial strategy. This multifaceted approach ensures the uniform saturation of the entire mould, effectively mitigating the formation of undesirable dry spots prior to the initiation of resin gelation [5]. A majority of composite parts are crafted using high-temperature curing resins, leading to the necessity of elevated mould temperatures. In practical industrial scenarios, these composite components are produced at higher mould temperatures to shorten the processing cycle. As the temperature rises, the resin undergoes chemical changes primarily through free radical polymerization, resulting in the creation of a three-dimensional network structure along with exothermic heat release [6]. Simultaneously, the resin undergoes a physical transformation from a liquid to a gel-like state and eventually solidifies into a rigid form due to cross-linking [7]. It's crucial to note that these chemical and physical alterations are closely interconnected and occur concurrently, influenced by both temperature and exothermic heat [8].

After reviewing the literature, it becomes evident that the optimization of mould-filling gate-vent placements and thermal-cure profiles has been addressed independently using both single and multi-objective optimization techniques. The widely

<sup>1</sup> CHEMICAL ENGINEERING, NATIONAL INSTITUTE OF TECHNOLOGY WARANGAL, TELANGANA, INDIA

<sup>2</sup> MECHANICAL ENGINEERING, MALLA REDDY ENGINEERING COLLEGE, INDIA

\* Corresponding author: [raghuraj@nitw.ac.in](mailto:raghuraj@nitw.ac.in)



employed optimization methods encompass the simplex method, genetic algorithm (GA), ant swarm strategy, non-dominated sorting genetic algorithm-II (NSGA-II), and the multi-objective optimization genetic algorithm (MOOGA) toolbox [9-13]. Objective functions focused on parameters such as process time, void content, weld lines, residual stresses, setup cost, temperature gradient, and more, were taken into consideration for optimizing the Resin Transfer Moulding (RTM) process [14,15].

In the work of Ye, Xugang et al. [16], a graph-based heuristic algorithm was developed for optimizing single gate and multiple vent locations across six different 2D geometries. Their approach involved fixing the gate location and then optimizing vent positions by minimizing the maximum distance between the gate and the vents. However, for larger and more complex structures, a solitary injection port might prove inadequate for achieving saturated mould fill within a minimal filling time. To address this, Liu et al. [17] introduced a hybrid simulated annealing genetic algorithm (SAGA) for optimizing the location of multiple mould gates, with the aim of enhancing convergence rates. They explored gate configurations ranging from two to five gates and compared the performance of SAGA against GA. The study revealed improved convergence rates with SAGA as the number of mould gates increased. J. Wang et al. [18] utilized the iterative Lloyd's algorithm to optimize multiple-gate injection based on the Centroidal Voronoi Diagram (CVD) approach. Their investigation demonstrated that the CVD method required fewer simulation runs to achieve minimal fill time compared to exhaustive search techniques and GA.

Shevtsov et al. [19] developed a curing model for a helicopter rotor blade within the COMSOL multi-physics simulator. They optimized the thermal profile for both solidification and liquefaction stages using a built-in optimization toolbox. However, this toolbox's capabilities were constrained to a limited selection of traditional optimization techniques, and results were influenced by initial assumptions, reducing their effectiveness. Furthermore, the toolbox lacked support for advanced hybrid multi-objective optimization methods. Jahromi et al. [20] devised an artificial neural network (ANN) toolbox to minimize temperature disparities between two designated points. The sequential quadratic programming (SQP) deterministic optimization technique was applied to ensure uniform temperature distribution and degree of cure across the thickness of the fibre-reinforced composite part. Yuan et al. [21] introduced a multi-objective strategy that integrated a multi-physics finite element process model with a radial basis function (RBF) surrogate model and NSGA-II to optimize the curing process for thick composites. They demonstrated the effectiveness of their optimization approach over the MRCC by comparing the obtained thermal-cure profiles.

In this work, an in-house coded cuckoo search (CS) optimization algorithm integrated with a finite element simulation model was developed for resin transfer moulding (RTM) process optimization. At first, the mould filling and curing phases, the vital stages of the RTM process were modelled in the COMSOL multi-physics simulator for RTM6 resin – carbon fibre reinforced composite part. Then, the model was imported to the CS opti-

mization algorithm scripted in MTALAB using the COMSOL live link for MATLAB. The CS algorithm was developed for the minimization of dry spot content by finding the optimal positions of gates and vents during the mould-filling stage and the minimization of the thermal gradient by finding the optimal mould temperature during the curing stage.

## 2. Materials and methodology

### 2.1. Raw materials

The resin matrix utilized in this study is RTM6 resin from Hexcel, an epoxy resin that has been meticulously degassed to ensure its purity. Tailored for advanced liquid composite moulding techniques, this mono component resin is well suited for the intended applications. As for the reinforcement material, a twill-weave carbon fibre mat with an areal density of 400 g/m<sup>2</sup> and a porosity of 46% was chosen as the primary reinforcement in this investigation.

### 2.2. Process models

The process models that simulate multi-phase fluid flow in porous media and resin cure kinetics of the RTM process using Darcy's law, the level set model and the thermochemical model were implemented as given below.

#### 2.2.1. Multi-phase fluid flow in porous media

The fluid flow through the porous media is modelled using Darcy's law as given in Eq. (1) and the associated flow mass balance is modelled using the continuity equation as given in Eq. (2). The level set model as given in Eq. (2) is used to track the flow front progression through the fibre preform.

$$\vec{u} = -\frac{\mathbf{K}}{\mu} \nabla P \quad (1)$$

$$\frac{\partial(\varnothing \rho_r)}{\partial t} + \nabla \cdot (\rho_r \vec{u}) = 0 \quad (2)$$

$$\frac{d\theta}{dt} + \vec{u} \cdot \nabla \theta = \gamma \nabla \cdot \left( \varepsilon \nabla \theta - \theta \frac{\nabla \theta}{|\nabla \theta|} \right) \quad (3)$$

where  $\vec{u}$  is the velocity vector,  $\varnothing$  is the porosity of the fibre mat,  $\rho_r$  is the density of resin,  $\mathbf{K}$  is the fibre mat permeability tensor,  $\nabla P$  is the pressure gradient and  $\mu$  is the viscosity of the resin. Also,  $\theta$ ,  $\varepsilon$ , and  $\gamma$  are the fluid volume function, the thickness of the interface and the initialization factor, respectively from the interface tracking level set model.

$$\text{Where } \theta \text{ is defined as, } \theta = \begin{cases} 0 & \text{resin unfilled domain} \\ (0,1) & \text{resin flow front} \\ 1 & \text{resin - saturated domain} \end{cases}$$

The boundary conditions associated with Eqs. (1-3) are given as,

$$\text{Mould-gate: } P = P_0$$

$$\text{Air-vent and resin flow interface: } P = 1 \text{ atmosphere}$$

$$\text{Mould boundary: } -n_r \cdot \rho_r \vec{u} = 0; n \cdot \left( \varepsilon \nabla \theta - \theta \frac{\nabla \theta}{|\nabla \theta|} \right) = 0$$

where  $P_0$  is the injection pressure of resin at the gate.

### 2.2.2. Thermochemical process model

In industrial practices, both the resin injection and mould are kept at elevated temperatures to enhance the porous media fluid flow and to reduce mould filling time. The transient energy balance for the cure analysis during mould filling that includes conduction, convection and resin cure is given in Eq. (4),

$$\begin{aligned} & (\varnothing \rho_r C_{Pr} + (1-\varnothing) \rho_f C_{Pf}) \frac{\partial T}{\partial t} + \\ & + \rho_r C_{Pr} (\vec{u} \cdot \nabla T) + \nabla \cdot (-k_c \nabla T) = \\ & = -\rho_r \varnothing \Delta H \frac{\partial \alpha}{\partial t} \end{aligned} \quad (4)$$

The thermal conductivity of the composite part is computed using the rule of mixture as given in Eq. (5),

$$k_c = \frac{k_r k_f}{k_r \varnothing + k_f (1-\varnothing)} \quad (5)$$

where  $\Delta H$  denotes the reaction heat and subscript 'r' and 'f' denotes the resin and fibre physical properties, respectively.

The resin cure kinetic model is demonstrated as follows,

$$\frac{d\alpha}{dt} = A e^{\frac{-E}{RT}} \alpha^m (1-\alpha)^n \quad (6)$$

The boundary conditions allied to address the Eqs. (4-6) are given as,

$$\text{Initial time } t = 0: T = T_0; \alpha = 0 \text{ and } \frac{d\alpha}{dt} = 0$$

$$\text{Mould boundary: } T = T_{mould};$$

$T_0$  denotes the initial temperature and  $T_{mould}$  denotes the mould temperature.

$E$  denotes activation energy,  $A$  denotes frequency factor,  $T$  denotes temperature,  $m$  and  $n$  denote the order of reaction and  $R$  denotes an ideal gas constant.

After completion of the mould-filling phase, the resin flow stops and therefore, the convection term from Eq. (4) is neglected during the curing process. The final condition of the mould-filling process is taken as the initial condition for the curing process and thus, the mould temperature profile is the only boundary condition required to simulate the resin cure process.

### 2.3. RTM Process Composite Parts

This study presents the development of the Resin Transfer Moulding (RTM) process specifically tailored for manufacturing composite parts using RTM6 resin and carbon fibre reinforcement. Figs. 1(a) and 1(b) illustrate the dimensions of the two-dimensional (2D) and three-dimensional (3D) plate structures, respectively. Tetrahedron mesh was employed for both composite plate structures in order to conduct process simulations. Mould-filling simulations for the composite plates were carried out with a constant resin injection pressure of  $4 \times 10^5$  Pa and resin injection temperatures set at  $120^\circ\text{C}$ . The mould filling simulations utilized 10 mm diameter mould gates and vents. The mathematical models, expressed in Eqs. (1-6) along with their respective initial and boundary conditions, were solved to facilitate the mould-filling simulations. Likewise, Eqs. (4-6) and their associated initial and boundary conditions were employed for the curing simulations. The parameters for RTM6 resin and carbon fibre, as well as their physical properties, were adopted from our previously published articles [22,23].

### 2.4. Methodology

The mould-filling and curing optimization was performed to obtain an effective injection strategy and optimal thermal-cure profile for the composite plates. The novel in-house coded cuckoo search (CS) optimization algorithm integrated with a finite element (FE) simulation model was developed in the COMSOL Livelink for MATLAB framework. The mould-filling optimization algorithm was performed to search for an optimal

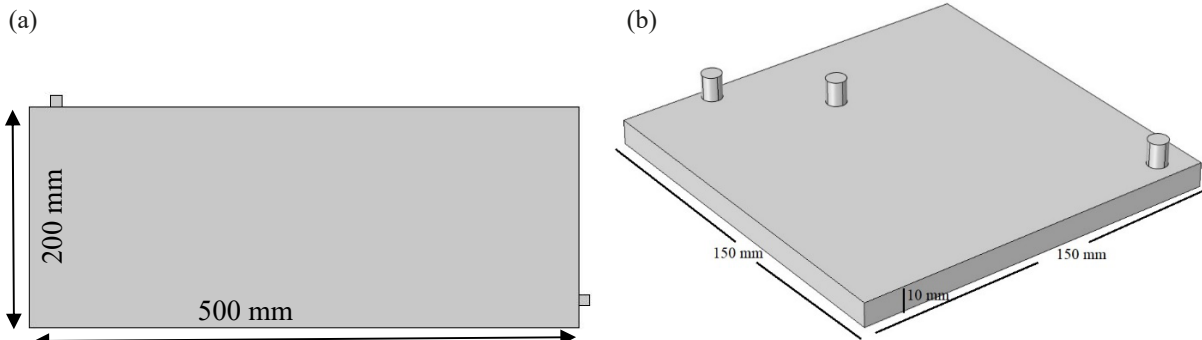


Fig. 1. (a) 2D Rectangular Plate, (b) 3D Rectangular Plate

position of injection ports and air vents by minimizing the dry spot content. The curing optimization was performed to search for an optimal mould temperature to obtain the minimum thermal gradient and cure time. The implementation and mathematical formulation of the CS algorithm and the proposed finite element simulation integrated cuckoo search (FE-CS) algorithm are discussed in the following subsections.

### 2.4.1. Cuckoo Search Optimization Algorithm

The cuckoo search algorithm operates as a stochastic, multi-start meta-heuristics optimization technique. In this approach, potential solutions are denoted as “cuckoo eggs.” Similar to the natural behaviour of cuckoos laying eggs in the nests of other birds, the CS algorithm simulates the process of discovering alien eggs by a host bird. The host bird may decide to either discard the foreign egg or abandon its nest to construct a new one elsewhere, influenced by a probability  $pa \in [0, 1]$ . Adhering to these principles, a novel solution is generated through a Lévy flight, employing randomly selected coordinates of an egg. This process is defined by the equation:

$$x_n^{t+1} = x_n + \beta \otimes \text{lévy}(\lambda) \tag{7}$$

Here,  $\otimes$  denotes entry-wise multiplication,  $\beta$  represents the step size, and  $\text{lévy}(\lambda)$  is a Lévy distribution. The step size  $\beta$  determines the scale of the random search, with its value contingent on the scale of the optimization problem. Typically, this parameter is set to 1 for most optimization problems [24]. An alternative expression for generating a new solution involves:

$$x_n^{t+1} = x_n^t - \beta(x_n^t - \text{bestnest}) \tag{8}$$

Where  $\beta$  is a constant, and the term in the brackets ensures the differentiation of two distinct random solutions. This formulation aims to prevent the detection of a high percentage of similar eggs [25].

In a real-world scenario, if a cuckoo’s egg closely resembles the host’s egg, the likelihood of its discovery diminishes. Consequently, a cuckoo’s egg can be updated through a biased random walk philosophy, described by the equation:

$$x_{new}^{t+1} = x_n^{t+1} + \text{rand} \times (x_2^{t+1} - x_1^{t+1}) \tag{9}$$

Here,  $\text{rand}$  is a uniformly distributed random number between 0 and 1. This process ensures that a cuckoo’s egg undergoes a random walk in a biased manner, further simulating the dynamics of real-world scenarios. The flow diagram of the cuckoo search algorithm is given in Fig. 2.

### 2.4.2. Mould-Filling Optimization Using Proposed FE-CS Optimization Algorithm

Initially, the FE-CS algorithm was developed to optimize the positions of injection ports and air vents. Many researchers used GA for optimizing the mould fill phase, however from the comparative studies, the CS algorithm has performed significantly better than GA for optimization problems [26]. Therefore in this work, the CS algorithm was developed for the mould fill and cure phases optimization of the RTM process. The optimization objective was considered the minimization of void content. Void content is the unsaturated area of resin in the composite part when the resin reaches the vents and it is calculated based on the total number of unfilled nodes using Eq. (10). The framed

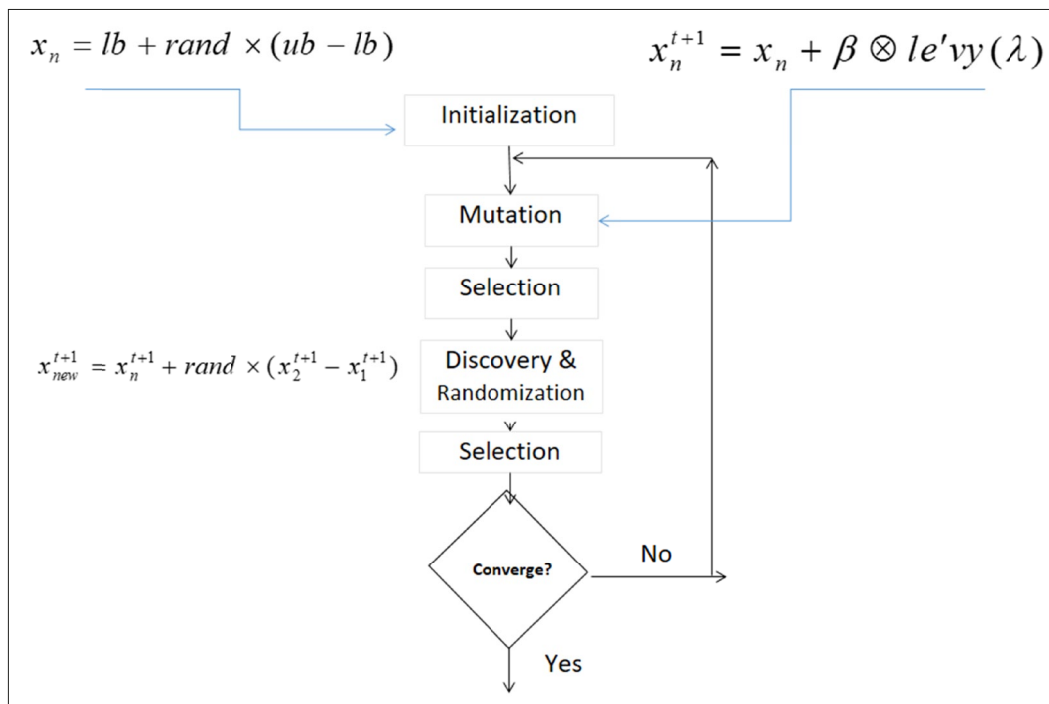


Fig. 2. Flow Diagram of Cuckoo Search Optimization Algorithm

objective was optimized by finding the optimum locations of gates and vents within the geometry search space  $R^D$ . The mathematical formulation of the optimization problem described above is given in Eq. (11).

$$\% \text{ Void Content} = \sum_{i=1}^{\text{total number of nodes}} \left( \frac{1 - \text{fill fraction of node } i}{\text{total number of nodes}} \right) \times 100 \quad (10)$$

$$\min f = \% \text{ Void content} \quad (11)$$

subject to

$$\text{Location of gates and vents} \in R^D$$

Where the objective function  $f$  is computed using Eq. (10) and optimized by changing the locations of gates and vents as design variable. Also, the locations of gates and vents were searched within the geometry search  $R^D$ . This optimization problem was implemented in MATLAB by combining the finite element (FE) simulation package using the COMSOL live link for MATLAB. Figs. 3 and 4 depict the flow diagram for the implementation of an in-house coded FE-CS algorithm to find the optimal positions of gates and vents. The tuning parameters  $\beta$  and  $pa$  were used as 1.5 and 0.25, respectively.

### 2.4.3. Cure Phase Optimization Using Proposed FE-CS Optimization Algorithm

The main objective of this optimization was to minimize the thermal gradient during the composite curing process. The thermal gradient was computed as the difference between the mould surface temperature ( $T_{max}$ ) and the composite panel mid-thickness temperature ( $T_{min}$ ). The curing optimization was

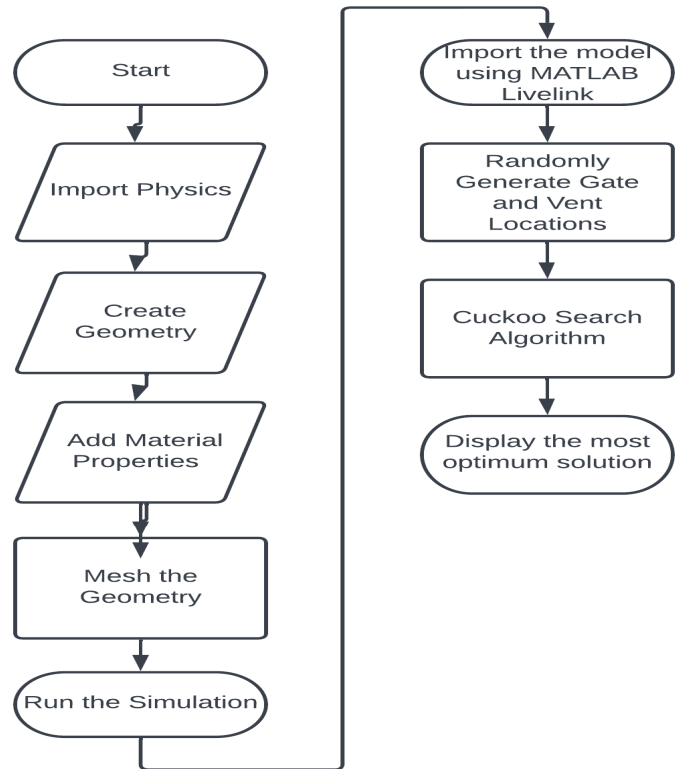


Fig. 3. Implementation of COMSOL Livelink for MATLAB Optimization Framework

performed to obtain the optimum mould heating profile with negligible temperature overshoot during the curing phase of the composite plates. The design variables mould temperature and cure time were varied within the given bounds as tabulated in TABLE 1. Also, the average degree of cure ( $\alpha_{avg}$ ) at the end of the curing process was constrained to 0.98 to ensure the composite part cure completion. The mathematical formulation for

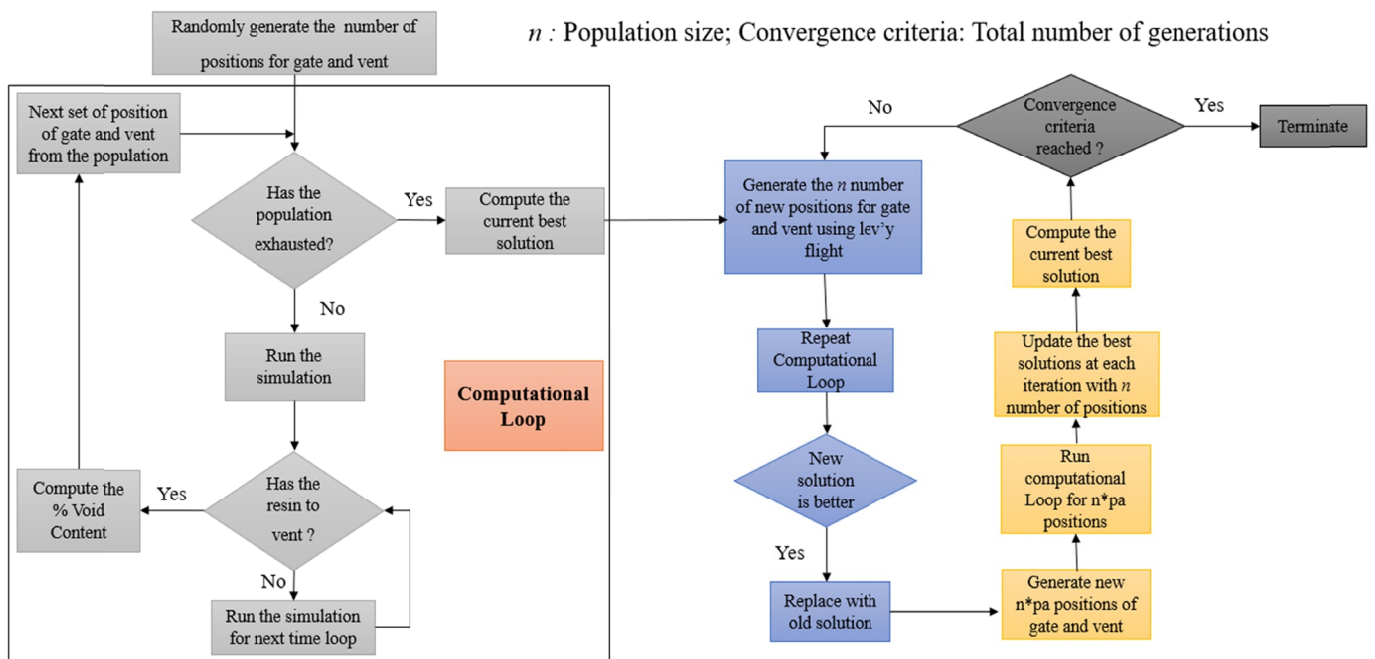


Fig. 4. Proposed FE-CS Optimization Algorithm for Mould-Filling Optimization



the curing phase optimization of the composite plate is given in Eq. (12). Fig. 5 depicts the flow diagram for the implementation of an in-house coded FE-CS algorithm to find the optimal mould temperature and cure time.

$$\min f = \sqrt[2]{\left[T_{\max\_domain}(t) - T_{\min\_domain}(t)\right]^2} \quad (12)$$

Subject to,

$$\alpha_{avg} \geq 0.98$$

$$t_1 \leq \text{Cure Time}(t) \leq t_2$$

$$T_1 \leq T_{mould} \leq T_2$$

TABLE 1

Design variables

Parameters	RTM6 Resin
$t_1$	50 min
$t_2$	300 min
$T_1$	433 K
$T_2$	493 K

## 2.5. Results and discussion

### 2.5.1. Mould-filling phase optimization

The primary goal of conducting mould-filling optimization is to identify an efficient injection strategy that utilizes the fewest gates and vents while achieving the shortest mould-fill time and preventing the formation of dry spots. Dry spots arise in

the mould-filling process when the resin front reaches the vents without adequately saturating the entire mould.

Initially, the positions of the gate (inlet) and vent (outlet) were optimized using the CS algorithm for a 2D rectangular composite plate with a pre-determined injection strategy involving one gate and one vent. A population size of 5 and 10 generations was employed for the iterative simulation runs.

TABLE 2 presents the optimal solutions obtained for varying positions of the gate and vent in the 2D rectangular composite plate. The resin-filled area is depicted in dark red, while the unfilled dry spot area is shown in blue on the surface plots in TABLE 2. The results indicate that void content decreased with an increase in generations. The optimal positions for the gate-vent were identified within 5 generations, achieving a 3% void content. The fill percentage for this configuration reached 97%, and the simulation was completed in 40 seconds. The optimal gate coordinates were (0 mm, 100 mm), and the vent coordinates were (500 mm, 50 mm). Beyond 5 generations, no significant changes in void content were observed; therefore, the optimization process was terminated after the 5<sup>th</sup> generation.

Subsequently, the positions of the gates (inlet) and vent (outlet) were optimized using the CS algorithm for a 3D rectangular composite plate with a pre-determined injection strategy involving two gates and one vent. A population size of 5 and 10 generations was employed for the iterative simulation runs. TABLE 3 presents the optimal solutions obtained for varying positions of the gate and vent in the 3D composite plate. The resin-filled area is depicted in dark red, while the unfilled dry spot area is shown in blue on the surface plots in TABLE 3. The results indicate that void content decreased with an increase

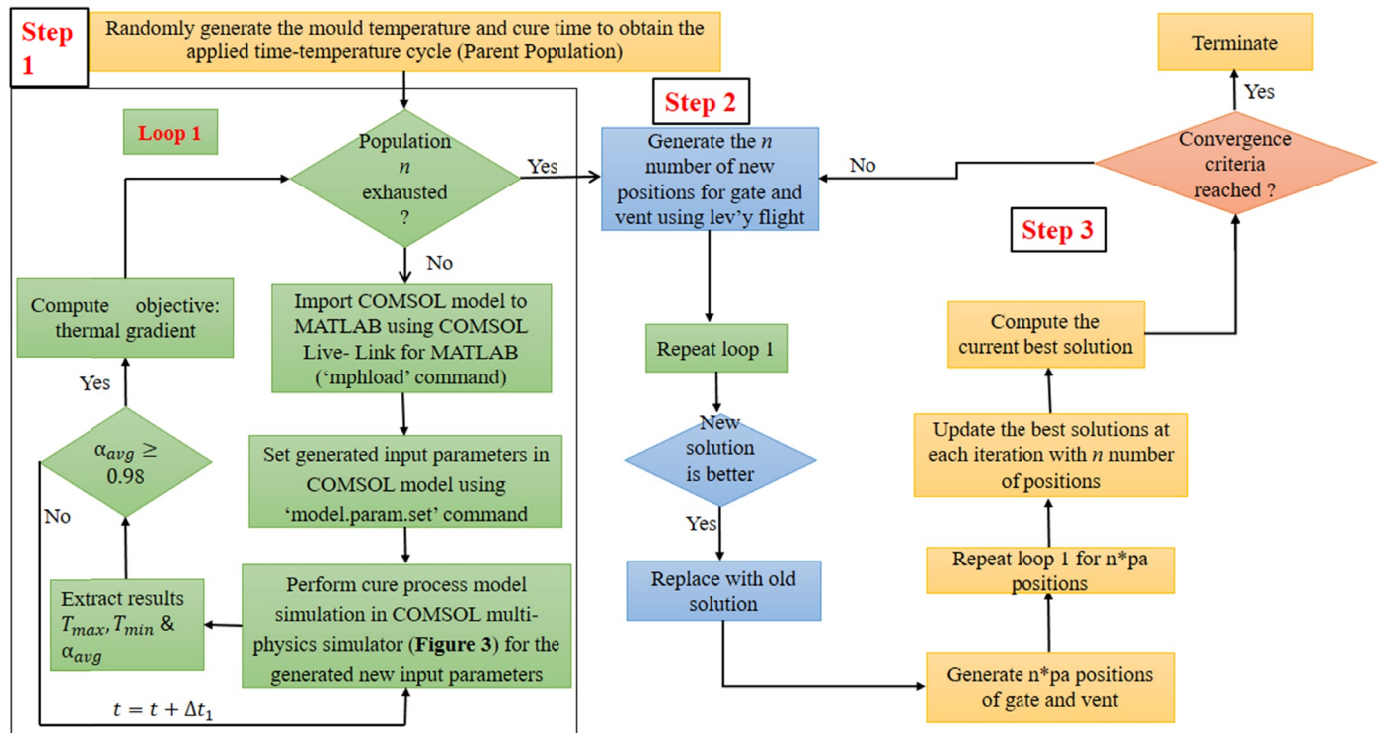
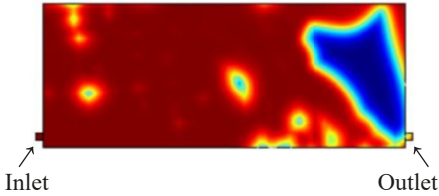






Fig. 5. Proposed FE-CS Optimization Algorithm for Cure Phase Optimization

TABLE 2

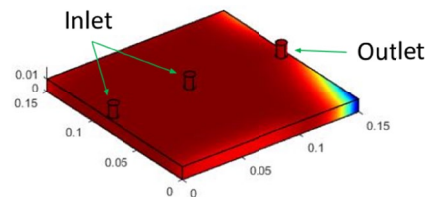
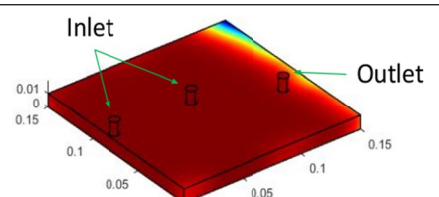
Optimal Positions of Gate and Vent with Generations for 2D Composite Plate

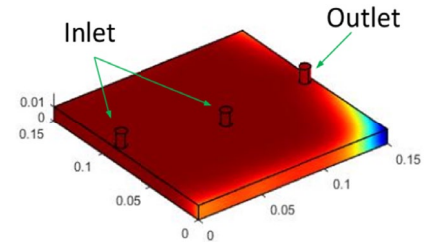
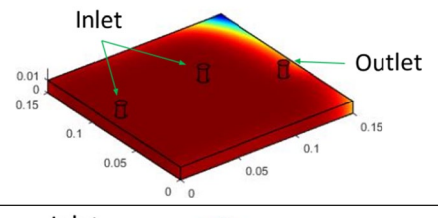
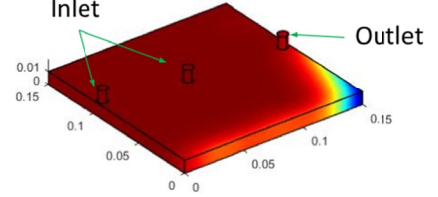
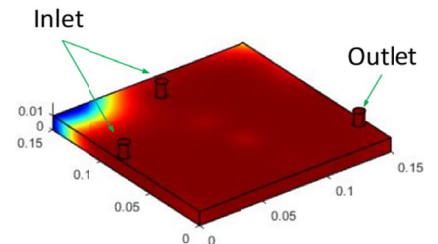
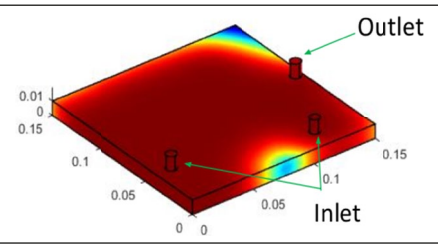
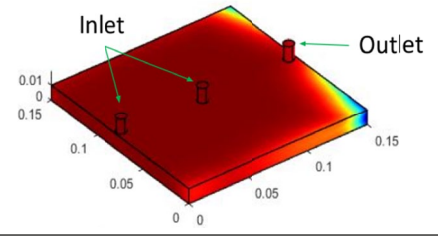
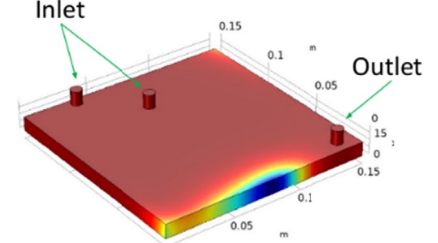
Generation No.	Flow Front	% Void Content
1		22%
2		17%
3		15%
4		9%
5		3%

in generations as shown in Fig. 6. The optimal positions for the gate-vent were identified within 7 generations, achieving a 0.56% void content. Beyond 7 generations, no significant changes in void content were observed as can be seen in Fig. 6.

TABLE 3

Optimal Positions of Gate and Vent with Generations for 3D Composite Plate

Generation	Flow Front	% Void Content
1		1.73
2		1.13

3		0.83
4		0.59
5		0.59
6		0.56
7		0.56
8		0.56
9		0.56

2.5.2. Curing phase optimization

The primary goal of optimizing the cure phase is to achieve the completion of the composite part cure in the shortest possible

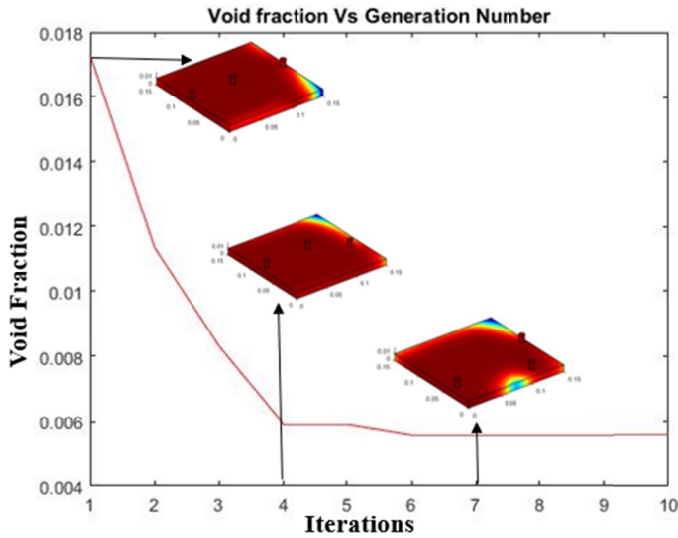


Fig. 6. Void Fraction vs. Iterations

cure time while minimizing thermal gradients. The optimization of the cure process was conducted using the developed FE-CS algorithm for a 3D composite plate. In Fig. 7, the optimization results are presented, illustrating the relationship between thermal gradient and the number of iterations. The results indicate a decrease in thermal gradient values with an increase in the number of iterations. Notably, during the 2<sup>nd</sup> iteration, the thermal gradient value significantly decreased due to the exploration capability of the CS algorithm. However, to ensure consistent convergence in solutions, we iterated until completing 10 iterations. From the results, it is evident that the thermal gradient value remained stable until the 8<sup>th</sup> iteration, with a slight decrease observed at the 9<sup>th</sup> iteration before stabilizing again. Since there was no significant change in the thermal gradient after the 9<sup>th</sup> iteration, the final optimal results obtained at the 10<sup>th</sup> iteration are summarized in TABLE 4. From TABLE 4, it is observed that the minimum thermal gradient value was achieved at 0.86 K, corresponding to a mould temperature of 433 K. To attain this minimum thermal gradient value and achieve a degree of cure of 98.15%, a cure time of 250 minutes was required.

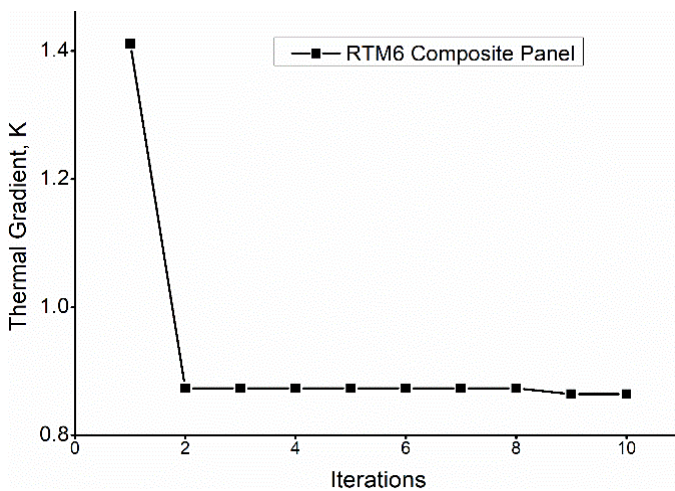


Fig. 7. Thermal Gradient vs. Iterations

TABLE 4

Optimal Parameters obtained using FE-CS Algorithm

Parameters	RTM6 resin
Mould Temperature	433.0858 K
Thermal Gradient	0.8642 K
Cure Time	250 min
Average Degree of Cure	0.9815

From these findings, it is evident that achieving a lower thermal gradient comes at the expense of requiring a longer cure time. Consequently, to strike a balance between cure time and thermal gradient, we have devised a multi-objective optimization problem. This problem aims to simultaneously minimize the thermal gradient and cure time, with the inclusion of constraints on the degree of cure and mould temperature as design variables, as expressed in Eq. (13).

$$\min f_1 = \sqrt[2]{[T_{\max\_domain}(t) - T_{\min\_domain}(t)]^2} \quad (13)$$

$$\text{Min } f_2 = \text{Cure Time } (t)$$

Subject to,

$$\alpha_{avg} \geq 0.98$$

$$T_1 \leq T_{mould} \leq T_2$$

Fig. 8 depicts the Pareto front representing the trade-off relationship between thermal gradient and cure time for the 3D composite plate. The Pareto optimal front in Fig. 8 takes the form of an L-shaped curve, comprising three distinct regions: (i) the vertical segment, indicating a substantial change in thermal gradient values with a minor alteration in cure time; (ii) the horizontal segment, denoting a significant change in cure time with slight variations in thermal gradient values; and (iii) the curved region, representing a favourable equilibrium between thermal gradient and curing time. In addition, Fig. 8 illustrates the impact of mould temperature on the Pareto front between thermal gradient and cure time at generation 5 with a population

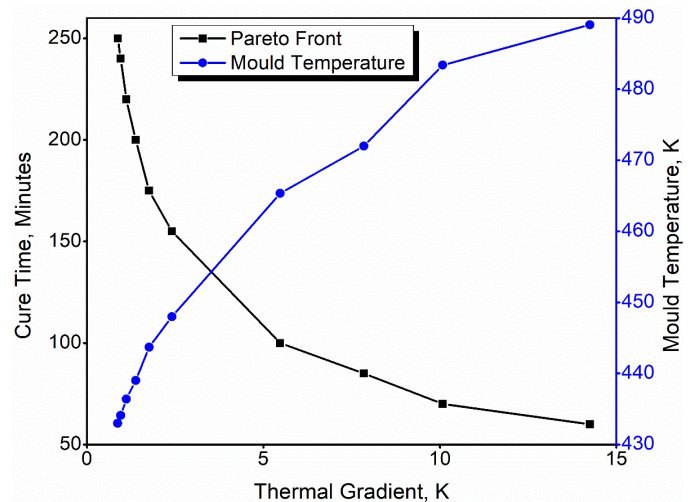


Fig. 8. Effect of Mould Temperature on the Pareto Front between Thermal Gradient and Cure Time



size of 10. The results reveal a clear correlation: a decrease in thermal gradient corresponds to an increase in cure time, and vice versa. The extreme values for thermal gradients range from 0.08 K to 14.9 K, while the cure time spans from 50 minutes to 250 minutes.

Fig. 9 illustrates the simulation results at one of the Pareto optimal points corresponding to a mould temperature of 470 K. Figs. 9(a) and 9(b) display the variations in temperature and degree of cure at different points along the thickness direction inside the composite plate. These points are strategically chosen to observe the overall variations in temperature and degree of cure over time in the composite plate. Points A and G are positioned close to the mould wall on the top and bottom sides, while the other points are situated between these two extremes. Initially, the cure conversion is sluggish, remaining below 5% within the first 10 minutes. The initial slow cure conversion during the first 10 minutes can be attributed to the reaction taking appreciable time to occur at lower temperatures. Once the temperature rises to a significant value, the rate of cure conversion starts accelerating with time until the curing process reaches completion.

### 3. Conclusion

In conclusion, this research presents the successful integration of an in-house coded Cuckoo Search (CS) optimization algorithm with a finite element simulation model for the optimization of the resin transfer moulding (RTM) process. The critical stages of mould filling and curing in the RTM process were initially modelled using the COMSOL Multi-Physics simulator for a composite part consisting of RTM6 resin and carbon fibre reinforcement. Subsequently, the model was imported into the CS optimization algorithm developed in MATLAB using the COMSOL Live Link for MATLAB.

The CS algorithm was specifically tailored for minimizing dry spot content during the mould-filling stage and reducing thermal gradient during the curing stage. Optimization results revealed a consistent decrease in dry spot content and thermal

gradient with an increase in generations. Converged, stable, and optimal solutions were achieved over successive generations. Notably, a dry spot content of 3% for a single injection port and one vent, and 0.56% for two injection ports and one vent were attained for two-dimensional and three-dimensional composite plates, respectively. In the context of curing phase optimization, the developed CS algorithm yielded a minimum thermal gradient of 0.86 K with a degree of cure of 98.1% for the optimal mould temperature of 433 K. To achieve a uniform balance between thermal gradient and cure time, a multi-objective optimization problem was addressed, and the Pareto front between thermal gradient and cure time was obtained. These results indicate that the CS algorithm effectively predicted superior automated mould-fill and cure phase optimal solutions for the studied composite part. Overall, the integration of the CS optimization algorithm with finite element simulation demonstrates its capability to enhance the efficiency and performance of the RTM process for composite manufacturing.

### REFERENCES

- [1] S.G. Advani, M.E. Sozer, *Process Modeling in Composites Manufacturing*, (2003).
- [2] Y.K. Hamidi, M.C. Altan, *Process Induced Defects in Liquid Molding Processes of Composites*. *Int. Polym. Process.* **32**, 527-544 (2017).
- [3] A. Zade, R.R.P. Kuppusamy, *A review on numerical optimization in liquid composite moulding processes*. *Mater. Today Proc.* **19**, 329-332 (2019). DOI: <https://doi.org/10.1016/j.matpr.2019.07.605>
- [4] C.H. Park, A. Lebel, A. Saouab, J. Bréard, W. Il Lee, *Modeling and simulation of voids and saturation in liquid composite molding processes*. *Compos. Part A.* **42**, 658-668 (2011). DOI: <https://doi.org/10.1016/j.compositesa.2011.02.005>
- [5] B.X. Chai, B. Eisenbart, M. Nikzad, B. Fox, A. Blythe, P. Blanchard, J. Dahl, *Simulation-based optimisation for injection configuration design of liquid composite moulding processes: A review*. *Compos. Part A Appl. Sci. Manuf.* **149**, 106540 (2021). DOI: <https://doi.org/10.1016/j.compositesa.2021.106540>

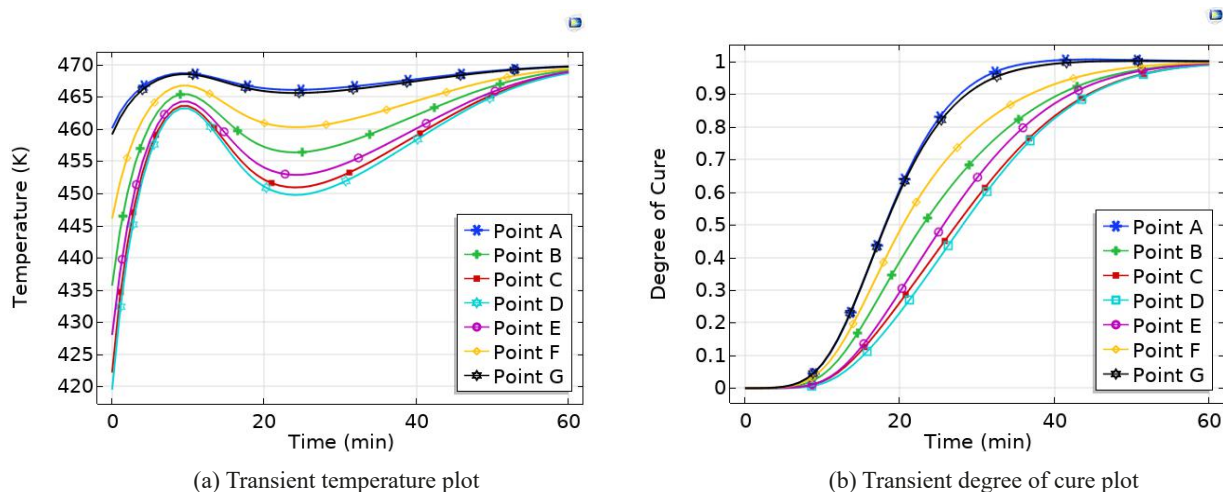


Fig. 9(a & b). Temperature and Degree of Cure Variation at Different Points along the Thickness Direction of Composite Plate

- [6] X. Hui, Y. Xu, W. Zhang, W. Zhang, Cure process evaluation of CFRP composites via neural network: From cure kinetics to thermochemical coupling. *Compos. Struct.* **288**, 115341 (2022). DOI: <https://doi.org/10.1016/j.compstruct.2022.115341>
- [7] D. Dolkun, H. Wang, H. Wang, Y. Ke, An efficient thermal cure profile design method for autoclave curing of large size mold. *Int. J. Adv. Manuf. Technol.* **114**, 2499-2514 (2021). DOI: <https://doi.org/10.1007/s00170-021-07015-4>
- [8] R. Matsuzaki, R. Yokoyama, T. Kobara, T. Tachikawa, Multi-Objective Curing Optimization of Carbon Fiber Composite Materials Using Data Assimilation and Localized Heating. *Compos. Part A.* **119**, 61-72 (2019). DOI: <https://doi.org/10.1016/j.compositesa.2019.01.021>
- [9] E. Ruiz, F. Trochu, Comprehensive Thermal Optimization of Liquid Composite Molding to Reduce Cycle Time and Processing Stresses. *Polym. Compos.* (2005). DOI: <https://doi.org/10.1002/pc.20077>
- [10] P. Carlone, G.S. Palazzo, A Simulation Based Metaheuristic Optimization of the Thermal Cure Cycle of Carbon-Epoxy Composite Laminates. In: *AIP Conf. Proc.*, (2014). DOI: <https://doi.org/10.1063/1.3589483>
- [11] V. Achim, F. Ratle, F. Trochu, Evolutionary operators for optimal gate location in liquid composite moulding. *Appl. Soft Comput.* **9**, 817-823 (2009). DOI: <https://doi.org/10.1016/j.asoc.2008.05.008>
- [12] I.V. Tarasov, S.N. Shevtsov, V. Evlanov, E.E. Orozaliev, V. Tarasov, V. Evlanov, Model-Based Optimal Control of Polymeric Composite Cure in Autoclave System. In: *IFAC-PapersOnLine*, Elsevier Ltd., p. 204-210 (2015). DOI: <https://doi.org/10.1016/j.ifacol.2015.09.184>
- [13] G. Struzziero, A.A. Skordos, Multi-objective optimisation of the cure of thick components. *Compos. Part A.* **93** (2016). DOI: <https://doi.org/10.1016/j.compositesa.2016.11.014>
- [14] J. Wang, P. Simacek, S.G. Advani, Use of medial axis to find optimal channel designs to reduce mold filling time in resin transfer molding. *Compos. Part A Appl. Sci. Manuf.* **95**, 161-172 (2017). DOI: <https://doi.org/10.1016/j.compositesa.2017.01.003>
- [15] G. Struzziero, Optimisation of the VARTM process. (2015). DOI: <https://doi.org/10.13140/RG.2.1.4994.9921>
- [16] X. Ye, C. Zhang, Z. Liang, B. Wang, Heuristic Algorithm for Determining Optimal Gate and Vent Locations for RTM Process Design. *J. Manuf. Syst.* **23** (2004).
- [17] J. Liu, J. Xie, L. Chen, A hybrid optimization algorithm for gate locations in the liquid composite molding process. *Text. Res. J.* **1-9** (2022). DOI: <https://doi.org/10.1177/00405175221109625>
- [18] J. Wang, P. Simacek, S.G. Advani, Composites: Part A Use of Centroidal Voronoi Diagram to find optimal gate locations to minimize mold filling time in resin transfer molding. *Compos. Part A.* **87**, 243-255 (2016). DOI: <https://doi.org/10.1016/j.compositesa.2016.04.026>
- [19] S.N. Shevtsov, I. Zhilyaev, I.A. Parinov, Optimization of the Composite Cure Process Based on the Thermo-Kinetic Model. *Adv. Mater. Res.* **569**, 185-192 (2012). DOI: <https://doi.org/10.4028/www.scientific.net/AMR.569.185>
- [20] P.E. Jahromi, A. Shojaei, S.M.R. Pishvaie, Prediction and optimization of cure cycle of thick fiber-reinforced composite parts using dynamic artificial neural networks. *J. Reinf. Plast. Compos.* **31**, 1201-1215 (2012). DOI: <https://doi.org/10.1177/0731684412451937>
- [21] Z. Yuan, L. Kong, D. Gao, X. Tong, Y. Feng, G. Yang, Z. Yang, S. Li, Multi-objective approach to optimize cure process for thick composite based on multi-field coupled model with RBF surrogate model. *Compos. Commun.* **24**, 100671 (2021). DOI: <https://doi.org/10.1016/j.coco.2021.100671>
- [22] A. Zade, S. Neogi, R.R.P. Kuppusamy, Design of effective injection strategy and operable cure window for an aircraft wing flap composite part using neat resin characterization and multi-physics process simulation. *Polym. Compos.* **43**, 3426-3445 (2022). DOI: <https://doi.org/https://doi.org/10.1002/pc.26626>
- [23] A. Zade, S. Neogi, R.R.P. Kuppusamy, Development of non-dominated sorting differential evolution algorithm for cure cycle optimization of industrial composite parts. *J. Reinf. Plast. Compos.* **07316844231212527** (2023). DOI: <https://doi.org/10.1177/07316844231212527>
- [24] X.-S. Yang, S. Deb, Cuckoo search via Lévy flights. In: *2009 World Congr. Nat. Biol. Inspired Comput.* 210-214 (2009).
- [25] X.-S. Yang, S. Deb, Multiobjective cuckoo search for design optimization. *Comput. Oper. Res.* **40**, 1616-1624 (2013).
- [26] M. Köppen, K. Yoshida, Evolutionary Multi-Criterion Optimization. *Evol. Multi-Criterion Optim.* **4403**, 727-741 (2007). DOI: <https://doi.org/10.1007/978-3-540-70928-2>